JEMAT 2022, Vol 10, No 2, 27-33
https://doi.org/10.54987/jemat.v10i2.770

HIBISCUS PUBLISHER

JOURNAL OF ENVIRONMENTAL MICROBIOLOGY AND TOXICOLOGY

Website: http://journal.hibiscuspublisher.com/index.php/JEMAT/index

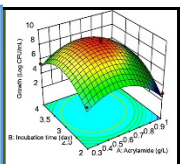

JEMAT VOL 10 NO 2 2022
RSM-Growth on acrylamide

Substrate Inhibition Kinetics Models for Fitting the Growth Rate of Phenol by an Immobilized *Pseudomonas putida*

Garba Uba[1]*, Hafeez Muhammad Yakasai[2] and Aisami Abubakar[3]

[1]Department of Science Laboratory Technology, College of Science and Technology, Jigawa State Polytechnic, Dutse, PMB 7040, Nigeria.
[2]Department of Biochemistry, College of Basic Medical science, Bayero University, Kano, PMB 3001- Nigeria.
[3]Department of Biochemistry, Faculty of science, Gombe State University, P.M.B 127, Tudun Wada, Gombe, Gombe State, Nigeria.

*Corresponding author:
Dr. Muhammad Hafeez Yakasai,
Department of Biochemistry, College of Basic Medical science,
Bayero University, Kano, PMB 3001- Nigeria.
Email: hmyakasai.bch@buk.edu.ng

HISTORY

Received: 12th Aug 2022
Received in revised form: 24th Oct 2022
Accepted: 5th Dec 2022

KEYWORDS

Substrate Inhibition Kinetics
Phenol
Pseudomonas putida
Immobilized bacterium
Teissier

ABSTRACT

Phenol, in particular, is one of several dangerous synthetic compounds created by humans. There were more than 80,000 chemicals produced in the US for industrial use, and many of these are phenol and phenolic compounds that end up in the environment without being subjected to adequate safety assessment. There are several types of bacteria that may use phenol as a carbon source, making bioremediation of this dangerous material a promising possibility. We found that at very high concentrations of phenol, the growth rate of *Pseudomonas putida* NAUN-16 was significantly slowed down. The primary growth model modified Gompertz was utilized to obtain the growth parameter specific growth rate. In this study, we continue the work by further modelling the effect of substrate or phenol on the growth rate of the bacterium using several substrate inhibition kinetic models such as Monod, Haldane, Teissier, Aiba, Yano and Koga, Han and Levenspiel, Luong, Moser, Webb and Hinshelwood. The resultant fittings show appreciable fitting with the exception of the Monod model. The Teissier model, as opposed to the more widely used Haldane model, better suited the growth rate data at different concentrations of phenol as judged by the results of the RMSE, AICc, adjustedR^2, F-test, and bias and accuracy factor. The designated values of the Teissier constants were maximal reduction rate, half saturation constant for maximal reduction and half inhibition constant which are symbolized by μ_{max}, K_s and K_i were 0.150 1/hr (95% confidence interval 0.120 to 0.180), 162.19 mg/L (95% C.I.55.58 to 268.79) and 1291.94 mg/L (95% C.I. 1067.24 to 1516.65), respectively. The value generated from curve fitting interpolation should not be taken as the actual value and it should be warned of this as the true μ_{max} should be where the gradient for the slope is zero and in this case the value was approximately 0.097 1/h at 385 mg/L phenol.

INTRODUCTION

Man-made synthetic chemicals, in particular, pose serious health risks. More than 80,000 chemicals were manufactured in the US for industrial purposes, and many more were released into the environment without proper safety testing. While it is true that the toxicity of naturally occurring and manmade chemicals cannot be compared, it is interesting to note that the five most poisonous substances on Earth are all naturally occurring [1]. The phenol industrial contaminant is between the most common, potentially hazardous substances come in essence as a result of industrialization[2]. Phenol contamination of Nigerian soils and water bodies have increased over the years, resulting in concern for its removal [3]. Numerous phenol-degrading bacteria from Nigeria have been isolated [4–7].

Inhalation and skin contact with phenol, which is extremely irritating to the skin, eyes, and mucous membranes, are the most common routes of phenol poisoning, which manifests itself acutely. In humans, the signs of acute poisoning include rapid heartbeat, shallow breathing, muscular weakness and tremors, loss of consciousness, and coma. Abnormal breathing, trembling and weakening of muscles, loss of coordination, convulsions, coma, and respiratory arrest are all symptoms of acute poisoning in humans. High acute toxicity from oral exposure to phenol has been seen in rodents, including rats, mice, and rabbits [8–11].

Chronic effects of phenol exposure in humans include a lack of appetite, gradual weight loss, diarrhea, dizziness, excessive salivation, and a dark urine color. Also noted are effects on the blood and liver, as well as gastrointestinal disturbances. One research indicated that following inhalation and cutaneous exposure to phenol and a few other chemicals, the subject had muscular soreness, weakness, an enlarged liver, and higher levels of liver enzymes. Topical phenol administration causes dermal irritation and necrosis. Humans exposed to extremely high levels of phenol have also shown cardiac arrhythmias. The central nervous system (CNS), kidneys, liver, lungs, and heart are all negatively impacted by prolonged inhalation of phenol in animals. Based on findings of decreased fetal body weights in rats, the Reference Dose for phenol is 0.6 mg/kg/d. The reference dose is an oral exposure estimate for the general population (including sensitive subgroups) that is expected to pose no significant risk of adverse noncancer consequences over the course of a lifetime (with uncertainty spanning possibly an order of magnitude). It is not a precise measure of danger, but rather a yardstick by which to evaluate outcomes. Potential for harmful health consequences to occur rises when exposures exceed the reference dosage. A lack of negative health effects does not always follow from a lifetime of exposure in excess of the reference dosage. Since the reference dose was derived from a study in which the dose was given via gavage, EPA has low confidence in that study; however, the database contains several supporting studies (subchronic, chronic, and reproductive/developmental), so EPA has medium confidence in the reference dose overall [8,12–16].

Workers who were exposed on the job reported small, statistically insignificant increases in the risk of developing specific malignancies, but the link between their exposure and their increased cancer risk was not established. Oral administration of phenol did not cause cancers in animals, but dermal application of phenol may promote tumor growth and/or be a weak skin carcinogen in mice. Despite this, the Environmental Protection Agency has placed phenol in Group D, "not classifiable as to human carcinogenicity," due to a dearth of information about its carcinogenic effects in both people and animals [17].

It is impossible to develop and optimize biological transformation processes without access to quantitative experimental data. Different mathematical models have been suggested to explain the metabolic dynamics of substances when they are exposed to either microorganism pure cultures or wild microbial populations. One useful tool in biotechnology is the relationship between the substrate concentration (S) and the specific growth rate (μ) of a microbial colony. In order to characterize the relationship between growth and substrate consumption rate, the Monod equation has been commonly employed [18,19]. The original Monod model, however, is useless when a substrate acts as an inhibitor of its own biodegradation. Instead, new constant-carrying derivatives have been developed to make substrate-related adjustments. In many different literatures, the Haldane model is used to represent substrate inhibition of growth or degradation rate.While other models have been proved to be more accurate when considering many substrate-inhibiting chemicals at once, such as phenol, this one continues to be used. As an illustration, the Haldane model isn't the only one out there [20], In addition to Luong's model, additional models have been proven to be superior [21,22] and Edward [23]. Therefore, in certain cases, the Haldane may be superseded by the use of the comprehensive models currently at hand. The Haldane model shouldn't be employed loosely without rigorous statistical examination and fitting alternative models to the existing growth or degradation rate data.

Previous research demonstrated that the primary growth models modified Gompertz and modified logistics were very close as the best models for fitting the growth of *Pseudomonas putida* (NAUN-16) on phenol [24]. In this study, we continue the work by further modelling the effect of substrate or phenol on the growth rate of the bacterium using several substrate inhibition kinetic models.

MATERIALS AND METHODS

Data from Fig 1. from the growth of *Pseudomonas putida* NAUN-16 on phenol [25] was processed using the software Webplotdigitizer 2.5 [26] which digitizes the scanned figure and has been utilized by many researchers and acknowledged for its reliability [27,28]. The modified Gompertz model from a previous work on refitting of this data [24] was utilized in this study (Eqn. 1). The ten models of inhibition kinetics are shown in **Table 1**.

$$y = A\left\{1 + v\exp(1+v)\exp\left[\frac{\mu_m}{A}(1+v)\left(1+\frac{1}{v}\right)(\lambda - t)\right]\right\}^{\left(\frac{-1}{v}\right)}$$
(Eqn. 1)

Table 1. Various mathematical models developed for degradation kinetics involving substrate inhibition of phenol on *Pseudomonas putida* (NAUN-16).

Author	Degradation Rate	Author
Monod	$\frac{\mu_{max}S}{S+K_s}$	[29]
Haldane	$\frac{\mu_{max}S}{S+K_s+\left(\frac{S^2}{K_i}\right)}$	[30]
Teissier	$\mu_{max}\left(1-\exp\left(-\frac{S}{K_i}\right)-\exp\left(\frac{S}{K_s}\right)\right)$	[31]
Aiba	$\mu_{max}\frac{S}{K_s+S}\exp\left(-\frac{S}{K_i}\right)$	[32]
Yano and Koga	$\frac{\mu_{max}S}{S+K_s+\left(\frac{S^2}{K_i}\right)\left(1+\frac{S}{K}\right)}$	[33]
Han and Levenspiel	$\mu_{max}\left(1-\left(\frac{S}{S_m}\right)\right)^n\left(\frac{S}{S+K_s\left(1-\left(\frac{S}{S_m}\right)\right)^m}\right)$	[34]
Luong	$\mu_{max}\frac{S}{S+K_s}\left(1-\left(\frac{S}{S_m}\right)\right)^n$	[35]
Moser	$\frac{\mu_{max}s^n}{K_s+s^n}$	[36]
Webb	$\frac{\mu_{max}S\left(1+\frac{S}{K}\right)}{S+K_s+\frac{S^2}{K_i}}$	[37]
Hinshelwood	$\mu_{max}\frac{S}{K_s+S}(1-K_pP)$	[38]

Note:
μ_{max} maximal specific growth rate
K_s half saturation constant
K_i inhibition constant
S_m maximal concentration of substrate tolerated
K_p product inhibition constant
m, n, K curve parameters
S substrate concentration
p product concentration

STATISTICAL ANALYSIS

Statistical significant difference between the models was calculated through various methods including the adjusted coefficient of determination (R^2), accuracy factor (AF), bias factor (BF), Root-Mean-Square Error (RMSE) and corrected AICc (Akaike Information Criterion) as before [27].

FITTING OF THE DATA

Fitting of the inhibition curves using various growth models was carried out using the CurveExpert Professional software (Version 1.6) by nonlinear regression utilizing the Marquardt algorithm.

Statistical analysis

Statistics functions such as adjusted coefficient of determination (R^2), Root-Mean-Square Error (RMSE), corrected AICc (Akaike Information Criterion), bias factor and accuracy factor (BF, AF) using the same set of experimental data, models with varying numbers of parameters were compared to one another to see if there was a significant difference in terms of fitness. The RMSE allows number of parameters' penalty and was calculated using Equation 1, where n illustrates the number of experimental data, where else p is the number of parameters calculated by the model and experimental data and values predicted by the model are Ob_i and Pd_i, respectively [39].

$$RMSE = \sqrt{\frac{\sum_{i=1}^{n}(Pd_i - Ob_i)^2}{n-p}} \qquad \text{(Eqn. 2)}$$

In linear regression, the best fitting model was determined by R^2 or coefficient of determination. However, in nonlinear regression, the R^2 does not give a comparative analysis where the number of parameters between models is different. To overcome this, adjusted R^2 was used to calculate the quality of the nonlinear models. In the adjusted R^2 formula, S_y^2 is the total variance of the y-variable and RMS is Residual Mean Square.

$$Adjusted\ (R^2) = 1 - \frac{RMS}{S_Y^2} \qquad \text{(Eqn. 3)}$$

$$Adjusted\ (R^2) = 1 - \frac{(1-R^2)(n-1)}{(n-p-1)} \qquad \text{(Eqn. 4)}$$

Using the Akaike Information Criterion (AIC), one can determine the relative quality of different statistical models for a given set of experimental data. Instead, data sets with many parameters or few values should use the corrected AIC, which is AICc [40]. The AICc was calculated based on the following Eqn. 4.

$$AICc = 2p + n1n\left(\frac{RSS}{n}\right) + 2(p+1) + \frac{2(p+1)(p+2)}{n-p-2} \qquad \text{(Eqn. 5)}$$

AICc provides information about the disparities in the number of parameters and the fitting between two models. The smallest AICc value would indicate the best fitting between the models [40].

Aside from AICc, Bayesian Information Criterion (BIC) (**Eqn. 5**) is another statistical method that is based on information theory. This error function penalizes the number of parameters more strongly than AIC [41].

$$BIC = n.\ln\frac{RSS}{n} + p.\ln(n) \qquad \text{(Eqn. 6)}$$

A further error function method based on the information theory is the Hannan–Quinn information criterion (HQC) (**Eqn. 6**). The HQC is strongly consistent unlike AIC due to the ln ln n term in the equation [42];

$$HQC = n \times ln\frac{RSS}{n} + 2 \times p \times ln(\ln n) \qquad \text{(Eqn. 7)}$$

The goodness-of-fit of the models was tested using BF and AF. In a molybdenum reduction, the Bias Factor should be equal to 1 to provide a perfect match between the predicted and observed value. The value of the Bias Factor (Eqn. 7) that is greater than 1 signifies a fail-safe model and a Bias Factor less than 1 indicates a fail-negative model. The value of Accuracy that ≥ 1 signifies less precise prediction (Eqn. 8).

$$Bias\ factor = 10\left(\sum_{i=1}^{n} log\frac{(Pd_i/Ob_i)}{n}\right) \qquad \text{(Eqn. 8)}$$

$$Accuracy\ factor = 10\left(\sum_{i=1}^{n} log\frac{|(Pd_i/Ob_i)|}{n}\right) \qquad \text{(Eqn. 9)}$$

RESULTS AND DISCUSSION

The modified Gompertz model was previously successfully used as a primary model to model the growth of the bacterium on phenol. There appears no or minimal lag period indicating the cellular machinery of the bacterium has been geared towards degradation and fast assimilation of toxic substances. This property of *Pseudomonas* spp. is well known as the genus of this bacterium is known for its ability to degrade toxic substances ranging from pesticides, hydrocarbons to pharmaceuticals [43–54]. In this investigation, we employed ten distinct substrate inhibition models for *Pseudomonas putida* NAUN-16 growth on phenol (**Table 1**). The standard substrate-based Monod model has the issue of overlooking the unique, regulatory complex, variable response to environmental stimuli, and the ability of microorganisms to create different products and by-products in intrinsic metabolism. The results of the RMSE, AICc, adjustedR^2, F-test, and bias and accuracy factor comparisons demonstrate that the Teissier model is the most accurate and precise of the kinetic models considered (**Table 2**). The resultant fittings (**Figs 2** to **11**) show appreciable fitting with the exception of the Monod model.

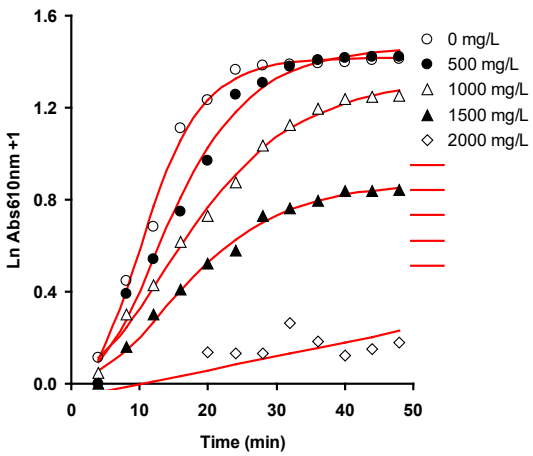

Fig 1. The growth curves of *P. putida* NAUN-16 on various concentrations of phenol as modelled using the modified Gompertz model.

https://doi.org/10.54987/jemat.v10i2.770

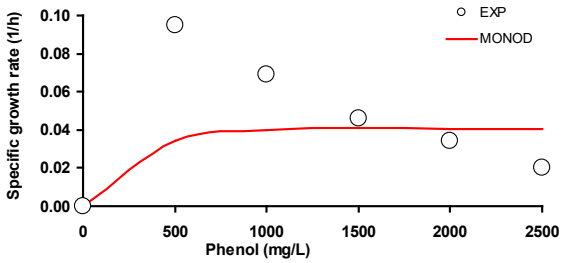

Fig 2. Resulting fitting of the specific growth data versus phenol concentration according to the model of Monod.

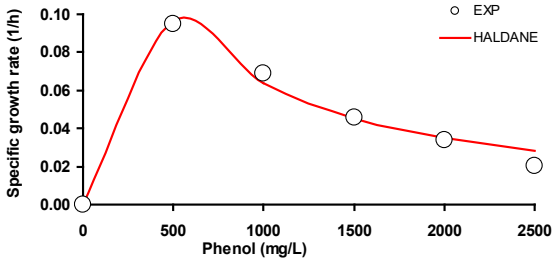

Fig 3. Resulting fitting of the specific growth data versus phenol concentration according to the model of Haldane.

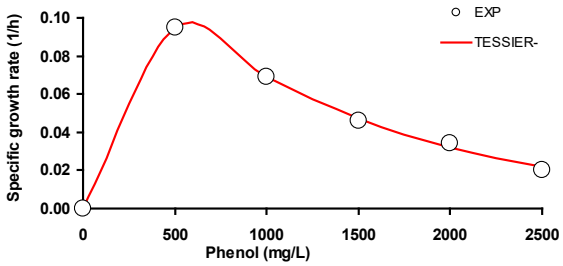

Fig 4. Resulting fitting of the specific growth data versus phenol concentration according to the model of Teissier.

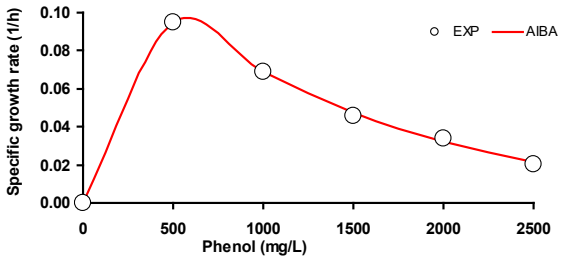

Fig 5. Resulting fitting of the specific growth data versus phenol concentration according to the model of Aiba.

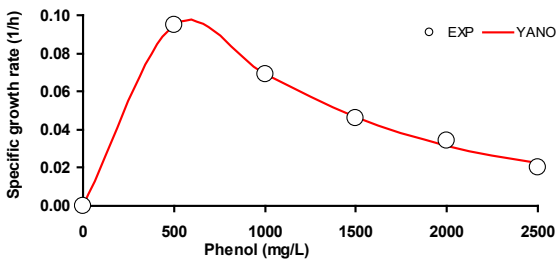

Fig 6. Resulting fitting of the specific growth data versus phenol concentration according to the model of Yano and Koga.

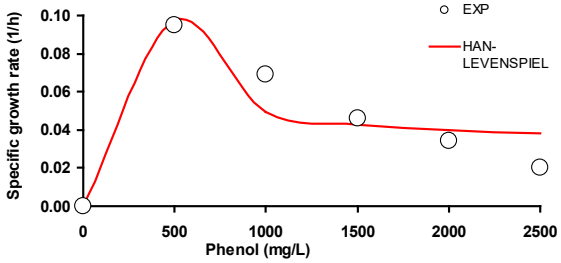

Fig 7. Resulting fitting of the specific growth data versus phenol concentration according to the model of Han and Levenspiel.

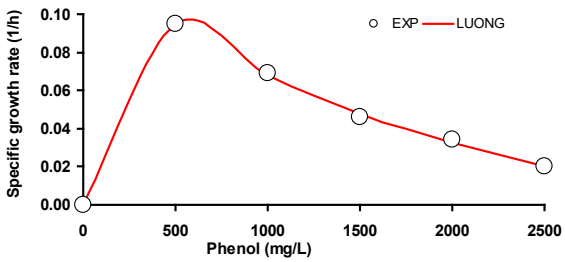

Fig 8. Resulting fitting of the specific growth data versus phenol concentration according to the model of Luong.

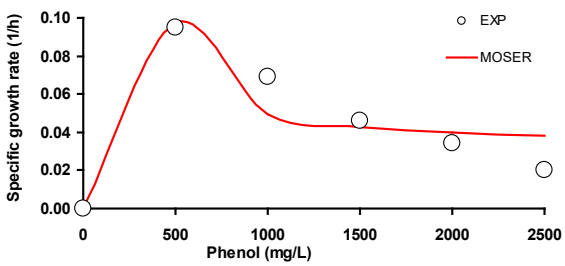

Fig 9. Resulting fitting of the specific growth data versus phenol concentration according to the model of Moser.

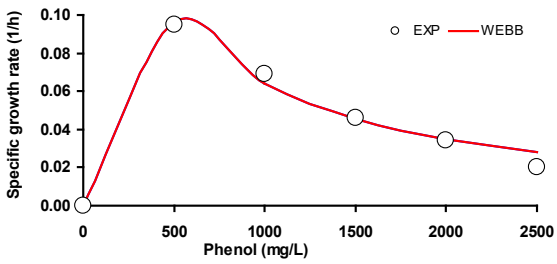

Fig 10. Resulting fitting of the specific growth data versus phenol concentration according to the model of Webb.

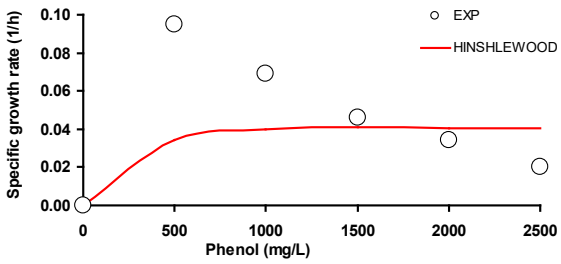

Fig 11. Resulting fitting of the specific growth data versus phenol concentration according to the model of Hinshelwood.

Table 2. Statistical analysis of the various fitting models.

Model	*p*	RMSE	adjR^2	AICc	BIC	HQC	BF	AF
Luong	4	0.00	1.00	-18.75	-88.97	-91.43	1.00	1.01
Yano	4	0.00	0.99	-15.93	-86.15	-88.61	1.01	1.03
Tessier-Edward	3	0.00	1.00	-62.50	-90.66	-92.51	1.00	1.02
Aiba	3	0.00	1.00	-62.56	-90.72	-92.57	1.00	1.02
Haldane	3	0.00	0.97	-44.77	-72.93	-74.77	1.04	1.07
Monod	2	0.03	-4.78	-32.67	-46.78	-48.01	0.89	1.24
Han and Levenspiel	5	0.02	0.06	n.a.	-54.24	-57.31	1.06	1.19
Moser	3	0.01	0.69	-30.12	-58.28	-60.12	1.06	1.19
Hinshlewood	4	0.04	-5.91	27.27	-42.94	-45.40	0.89	1.24
Webb	4	0.01	0.96	-1.67	-71.88	-74.34	1.04	1.07

Note:
p no of parameters
RMSE Root Mean Square Error
AdjR^2 Adjusted Coefficient of determination
BF Bias factor
AF Accuracy factor
n.a. not available

The designated values of the Teissier constants were maximal reduction rate, half saturation constant for maximal reduction and half inhibition constant which are symbolized by μ_{max}, K_s and K_i were 0.150 1/hr (95% confidence interval 0.120 to 0.180), 162.19 mg/L (95% C.I.55.58 to 268.79) and 1291.94 mg/L (95% C.I. 1067.24 to 1516.65), respectively. The value generated from curve fitting interpolation should not be taken as the actual value and it should be warned of this as the true μ_{max} should be where the gradient for the slope is zero and in this case the value was approximately 0.097 1/h at 385 mg/L phenol. The equation for the Teissier using the values obtained from the fitting is as follows;

$$\mu = 0.150\left(1 - exp\left(-\frac{S}{1291.94}\right) - exp\left(\frac{S}{162.19}\right)\right)$$

Because earlier models like Haldane's, Andrews and Noack's, Web's, and Yano's couldn't account for the extremely rare cases in which the growth rate turned zero at very high substrate concentrations, newer models like Luong's, Teissier's, and Hans Levenspiel's are created [55]. Substrate concentrations over a specific point can have repressive and toxic effects on microorganisms, slowing their development rate. Work on phenol-degrading microorganisms has been at the center of the bulk of Haldane model reports for xenobiotics-degrading bacteria to date [7,56–62]. The Teissier model has found applications in the modelling the degradation or growth rate of microbes on toxic xenobiotics [7,63–74]. The Teissier has been rarely used for modelling phenol inhibition of bacterial growth rates except in a few cases [6,6,64,75,76].

CONCLUSION

In this work, we found that *P. putida* NAUN-16's growth rate was strongly inhibited at extremely high concentrations of phenol, and that the Teissier model, as opposed to the more widely used Haldane model, better suited the growth rate data at different concentrations of phenol as judged by the majority of the discriminatory statistical results obtained.

REFERENCE

1. Özkara A, Akyil D, Konuk M. Pesticides, Environmental Pollution, and Health. In: Larramendy M, Soloneski S, editors. Environmental Health Risk - Hazardous Factors to Living Species. InTech; 2016 2020.
2. VanDoren PM. The Effects of Exposure to "Synthetic" Chemicals on Human Health: A Review. Risk Anal . 1996;16(3):367–76.
3. Ayeni O. A preliminary assessment of phenol contamination of Isebo River in south-western Nigeria. Greener J Phys Sci. 2014;4(2):30–7.
4. Agarry SE, Solomon BO. Kinetics of batch microbial degradation of phenols by indigenous *Pseudomonas fluorescence*. Int J Environ Sci Technol. 2008;5(2):223–32.
5. Agarry S e., Durojaiye A o., Yusuf R o., Aremu M o., Solomon B o., Mojeed O. Biodegradation of phenol in refinery wastewater by pure cultures of *Pseudomonas aeruginosa* NCIB 950 and Pseudomonas fluorescence NCIB 3756. Int J Environ Pollut. 2008 Jan;32(1):3–11.
6. Agarry SE, Solomon BO, Layokun SK. Substrate inhibition kinetics of phenol degradation by binary mixed culture of *Pseudomonas aeruginosa* and *Pseudomonas fluorescence* from steady state and wash- out data. Afr J Biotechnol. 2008;7(21):3927–33.
7. Agarry SE, Audu TOK, Solomon BO. Substrate inhibition kinetics of phenol degradation by *Pseudomonas fluorescence* from steady state and wash-out data. Int J Environ Sci Technol. 2009;6(3):443–50.
8. Bruce RM, Santodonato J, Neal MW. Summary Review of the Health Effects Associated With Phenol. Toxicol Ind Health. 1987 Oct 1;3(4):535–68.
9. Strikwold M, Spenkelink B, Woutersen RA, Rietjens IMCM, Punt A. Combining in vitro embryotoxicity data with physiologically based kinetic (PBK) modelling to define in vivo dose–response curves for developmental toxicity of phenol in rat and human. Arch Toxicol. 2013 Sep 1;87(9):1709–23.
10. Kottuparambil S, Kim YJ, Choi H, Kim MS, Park A, Park J, et al. A rapid phenol toxicity test based on photosynthesis and movement of the freshwater flagellate, *Euglena agilis* Carter. Aquat Toxicol. 2014 Oct 1;155:9–14.
11. Mohanta VL, Mishra BK. Occurrence and fate of phenolic compounds in groundwater and their associated risks. In: Legacy, Pathogenic and Emerging Contaminants in the Environment. CRC Press; 2021.
12. Kim JS, Chin P. Acute and chronic toxicity of phenol to mysid, Archaeomysis kokuboi. Korean J Fish Aquat Sci. 1995;28(1):87–97.
13. Abd Gami A, Shukor A, Yunus M, Abdul Khalil K, Dahalan FA, Khalid A, et al. Phenol and phenolic compounds toxicity. J Environ Microbiol Toxicol. 2014;2(1):11–23.
14. Gami AA, Shukor MY, Khalil KA, Dahalan FA, Khalid A, Ahmad SA. Phenol and its toxicity. J Environ Microbiol Toxicol. 2014;2(1):11–23.
15. Dhatwalia VK, Nanda M. Biodegradation of phenol: Mechanisms and applications. Toxicity and Waste Management Using Bioremediation. 2015. 198–214 p.
16. Duan W, Meng F, Cui H, Lin Y, Wang G, Wu J. Ecotoxicity of phenol and cresols to aquatic organisms: A review. Ecotoxicol Environ Saf. 2018;157:441–56.
17. US EPA R 05. Human Health Noncarcinogen Fact Sheet for Phenol: (Human Health Noncarcinogen - fish ingestion only), Wisconsin Department of Natural Resources . 2015
18. Kiviharju K, Salonen K, Leisola M, Eerikäinen T. Modeling and simulation of Streptomyces peucetius var. caesius N47 cultivation and ε-rhodomycinone production with kinetic equations and neural networks. J Biotechnol. 2006;126(3):365–73.
19. Shokrollahzadeh S, Bonakdarpour B, Vahabzadeh F, Sanati M. Growth kinetics and Pho84 phosphate transporter activity of Saccharomyces cerevisiae under phosphate-limited conditions. J Ind Microbiol Biotechnol. 2007;34(1):17–25.
20. Arif NM, Ahmad SA, Syed MA, Shukor MY. Isolation and characterization of a phenol-degrading Rhodococcus sp. strain AQ5NOL 2 KCTC 11961BP. J Basic Microbiol. 2013;53(1):9–19.
21. Hamitouche AE, Bendjama Z, Amrane A, Kaouah F, Hamane D. Relevance of the Luong model to describe the biodegradation of phenol by mixed culture in a batch reactor. Ann Microbiol. 2012;62(2):581–6.
22. Nickzad A, Mogharei A, Monazzami A, Jamshidian H, Vahabzadeh F. Biodegradation of phenol by Ralstonia eutropha in a Kissiris-immobilized cell bioreactor. Water Environ Res. 2012;84(8):626–34.
23. Saravanan P, Pakshirajan K, Saha P. Batch growth kinetics of an indigenous mixed microbial culture utilizing m-cresol as the sole carbon source. J Hazard Mater. 2009;162(1):476–81.
24. Uba G, Yakasai HM, Abubakar A. Mathematical modeling of the biodegradation of phenol from industrial effluents using

immobilized *Pseudomonas putida*. J Biochem Microbiol Biotechnol. 2020 Jul 31;8(1):15–8.
25. Singh U, Arora NK, Sachan P. Simultaneous biodegradation of phenol and cyanide present in coke-oven effluent using immobilized *Pseudomonas putida* and *Pseudomonas stutzeri*. Braz J Microbiol. 2018 Jan 1;49(1):38–44.
26. Rohatgi A. WebPlotDigitizer. http://arohatgi.info/WebPlotDigitizer/app/ Accessed June 2 2014.; 2015.
27. Halmi MIE, Shukor MS, Johari WLW, Shukor MY. Modeling the growth curves of *Acinetobacter* sp. strain DRY12 grown on diesel. J Environ Bioremediation Toxicol. 2014;2(1):33–7.
28. Khare KS, Phelan Jr FR. Quantitative comparison of atomistic simulations with experiment for a cross-linked epoxy: A specific volume–cooling rate analysis. Macromolecules. 2018;51(2):564–75.
29. Monod J. The Growth of Bacterial Cultures. Annu Rev Microbiol. 1949;3(1):371–94.
30. Boon B, Laudelout H. Kinetics of nitrite oxidation by Nitrobacter winogradskyi. Biochem J. 1962;85:440–7.
31. Teissier G. Growth of bacterial populations and the available substrate concentration. Rev Sci Instrum. 1942;3208:209–14.
32. Aiba S, Shoda M, Nagatani M. Kinetics of product inhibition in alcohol fermentation. Biotechnol Bioeng. 1968 Nov 1;10(6):845–64.
33. Yano T, Koga S. Dynamic behavior of the chemostat subject to substrate inhibition. Biotechnol Bioeng. 1969 Mar 1;11(2):139–53.
34. Han K, Levenspiel O. Extended Monod kinetics for substrate, product, and cell inhibition. Biotechnol Bioeng. 1988;32(4):430–7.
35. Luong JHT. Generalization of monod kinetics for analysis of growth data with substrate inhibition. Biotechnol Bioeng. 1987;29(2):242–8.
36. Moser A. Kinetics of batch fermentations. In: Rehm HJ, Reed G, editors. Biotechnology. VCH Verlagsgesellschaft mbH, Weinheim; 1985. p. 243–83.
37. Webb JLeyden. Enzyme and metabolic inhibitors . New York: Academic Press; 1963. 984 p. Available from: https://www.biodiversitylibrary.org/bibliography/7320
38. Hinshelwood CN. The chemical kinetics of the bacterial cell. Clarendon Press, Gloucestershire, UK; 1946.
39. Wayman M, Tseng MC. Inhibition-threshold substrate concentrations. Biotechnol Bioeng. 1976;18(3):383–7.
40. Głuszcz P, Petera J, Ledakowicz S. Mathematical modeling of the integrated process of mercury bioremediation in the industrial bioreactor. Bioprocess Biosyst Eng. 2011;34(3):275–85.
41. Kass RE, Raftery AE. Bayes Factors. J Am Stat Assoc. 1995 Jun 1;90(430):773–95.
42. Burnham KP, Anderson DR. Model Selection and Multimodel Inference: A Practical Information-Theoretic Approach. Springer Science & Business Media; 2002. 528 p.
43. Fritz H, Reineke W, Schmidt E. Toxicity of chlorobenzene on *Pseudomonas* sp. strain RHO1, a chlorobenzene-degrading strain. Biodegradation. 1991;2(3):165–70.
44. Saravanan P, Pakshirajan K, Saha P. Kinetics of phenol and m-cresol biodegradation by an indigenous mixed microbial culture isolated from a sewage treatment plant. J Environ Sci. 2008;20(12):1508–13.
45. Li L, Hong Q, Yan X, Fang G, Ali SW, Li S. Isolation of a malachite green-degrading *Pseudomonas* sp. MDB-1 strain and cloning of the tmr2 gene. Biodegradation. 2009;20(6):769–76.
46. Pathak H, Madamwar D. Biosynthesis of indigo dye by newly isolated naphthalene-degrading strain *Pseudomonas* sp. HOB1 and its application in dyeing cotton fabric. Appl Biochem Biotechnol. 2010;160(6):1616–26.
47. Hu J, Zhang LL, Chen JM, Liu Y. Degradation of paracetamol by *Pseudomonas aeruginosa* strain HJ1012. J Environ Sci Health - Part ToxicHazardous Subst Environ Eng. 2013;48(7):791–9.
48. Wang GL, Li XF, Zhang H, Xiong MH, Li F. Optimization of CTN-4 to chlorothalonil-degrading conditions and a kinetics model. Zhongguo Huanjing KexueChina Environ Sci. 2013;33(11):1999–2005.
49. Tiong B, Bahari ZM, Irwan SL, Jaafar J, Ibrahim Z, Shahir S. Cyanide degradation by *Pseudomonas pseudoalcaligenes* strain W2 isolated from mining effluent. Sains Malays. 2015;44(2):233–8.
50. Vignesh R, Arularasan A, V G, Deepika C. Isolation identification and characterization of potential oil degrading bacteria from oil contaminated sites. 2016 Jan 1;
51. Zhang C, Wang B, Dai X, Li S, Lu G, Zhou Y. Structure and function of the bacterial communities during rhizoremediation of hexachlorobenzene in constructed wetlands. Environ Sci Pollut Res. 2017 Apr 1;24(12):11483–92.
52. Habib S, Iruthayam A, Abd Shukor MY, Alias SA, Smykla J, Yasid NA. Biodeterioration of Untreated Polypropylene Microplastic Particles by Antarctic Bacteria. Polymers. 2020 Nov;12(11):2616.
53. Shettima H, Allamin IA, Halima N, Ismail HY, Musa Y. Isolation and Characterization of Hydrocarbon-degrading Bacteria in Soils of Mechanical Workshops in Maiduguri, Borno State. J Environ Bioremediation Toxicol. 2021 Dec 31;4(2):35–8.
54. Sufyan AJ, Ibrahim S, Babandi A, Yakasai HM. Characterization of Butachlor Degradation by A Molybdenum-Reducing and Aniline-degrading Pseudomonas sp. J Environ Microbiol Toxicol. 2021 Dec 31;9(2):8–12.
55. Saravanan P, Pakshirajan K, Saha P. Growth kinetics of an indigenous mixed microbial consortium during phenol degradation in a batch reactor. Bioresour Technol. 2008;99(1):205–9.
56. Kotturi G, Robinson CW, Inniss WE. Phenol degradation by a psychrotrophic strain of *Pseudomonas putida*. Appl Microbiol Biotechnol. 1991;34(4):539–43.
57. Bai J, Wen JP, Li HM, Jiang Y. Kinetic modeling of growth and biodegradation of phenol and m-cresol using Alcaligenes faecalis. Process Biochem. 2007;42(4):510–7.
58. Long TR, Zhang Z, Zhuan RX. Biodegradation of phenol by a novel isolated bacterium Pseudomonas sp. CN-6. Tumu Jianzhu Yu Huanjing Gongcheng Journal Civ Archit Environ Eng. 2010;32(5):82–7.
59. Liu J, Wang Q, Yan J, Qin X, Li L, Xu W, et al. Isolation and characterization of a novel phenol degrading bacterial strain WUST-C1. Ind Eng Chem Res. 2013;52(1):258–65.
60. Basak SP, Sarkar P, Pal P. Isolation and characterization of phenol utilizing bacteria from industrial effluent-contaminated soil and kinetic evaluation of their biodegradation potential. J Environ Sci Health A Tox Hazard Subst Environ Eng. 2014;49(1):67-77.
61. Ding C, Wang Z, Cai W, Zhou Q, Zhou J. Biodegradation of phenol with Candida tropicalis isolated from aerobic granules. Fresenius Environ Bull. 2014;23(3 A):887–95.
62. Mohanty SS, Jena HM. Biodegradation of phenol by free and immobilized cells of a novel Pseudomonas sp. nbm11. Braz J Chem Eng. 2017 Mar;34:75–84.
63. Kiviharju K, Salonen K, Leisola M, Eerikäinen T. Modeling and simulation of Streptomyces peucetius var. caesius N47 cultivation and ε-rhodomycinone production with kinetic equations and neural networks. J Biotechnol. 2006;126(3):365–73.
64. Agarry SE, Solomon BO. Kinetics of batch microbial degradation of phenols by indigenous *Pseudomonas fluorescence*. Int J Environ Sci Technol. 2008;5(2):223–32.
65. Annuar MSM, Tan IKP, Ibrahim S, Ramachandran KB. A kinetic model for growth and biosynthesis of medium-chain-length poly-(3-hydroxyalkanoates) in *Pseudomonas putida*. Braz J Chem Eng. 2008 Jun;25(2):217–28.
66. Singh RK, Kumar S, Kumar S, Kumar A. Biodegradation kinetic studies for the removal of p-cresol from wastewater using *Gliomastix indicus* MTCC 3869. Biochem Eng J. 2008;40(2):293–303.
67. Sack ELW, van der Wielen PWJJ, van der Kooij D. Flavobacterium johnsoniae as a model organism for characterizing biopolymer utilization in oligotrophic freshwater environments. Appl Environ Microbiol. 2011;77(19):6931–8.
68. del Barrio MC, Demafelis RB, Mercado SM, Movillon JL, Rebancos CM. Growth kinetics of *Rhizopus chinensis* Saito BIOTECH 3273 in the production of microbial rennet using coconut paring cake as substrate. Philipp Agric Sci Philipp . 2012 [cited 2020 Dec 20]; Available from: https://agris.fao.org/agris-search/search.do?recordID=PH2014000116
69. Tavassoli T, Mousavi SM, Shojaosadati SA, Salehizadeh H. Asphaltene biodegradation using microorganisms isolated from oil samples. Fuel. 2012 Mar 1;93:142–8.
70. Gharibzahedi SMT, Razavi SH, Mousavi M. Kinetic analysis and mathematical modeling of cell growth and canthaxanthin

biosynthesis by *Dietzia natronolimnaea* HS-1 on waste molasses hydrolysate. RSC Adv. 2013;3(45):23495–502.

71. Vijayalakshmi V, Senthilkumar P, Mophin-Kani K, Sivamani S, Sivarajasekar N, Vasantharaj S. Bio-degradation of Bisphenol A by *Pseudomonas aeruginosa* PAb1 isolated from effluent of thermal paper industry: Kinetic modeling and process optimization. J Radiat Res Appl Sci. 2018 Jan 1;11(1):56–65.
72. Zhao H, Zhu J, Liu S, Zhou X. Kinetics study of nicosulfuron degradation by a Pseudomonas nitroreducens strain NSA02. Biodegradation. 2018;29(3):271–83.
73. Uba G, Abubakar A, Ibrahim S. Optimization of Process Conditions for Effective Degradation of Azo Blue Dye by *Streptomyces* sp. DJP15: A Secondary Modelling Approac. Bull Environ Sci Sustain Manag. 2021 Dec 31;5(2):28–32.
74. Najim AA, Ismail ZZ, Hummadi KK. Immobilization of mixed bacteria by novel biocarriers extracted from Cress and Chia seeds for biotreatment of anionic surfactant (SDS)-bearing real wastewaters. Prep Biochem Biotechnol. 2022;
75. Begum SS, Radha KV. Investigating the performance of inverse fluidized bed biofilm reactor for phenol biodegradation using Pseudomonas fluorescence. In: Proceedings of the International Conference on Green Technology and Environmental Conservation, GTEC-2011. 2011. p. 130–6.
76. Halmi MIE, Shukor MS, Johari WLW, Shukor MY. Mathematical modelling of the degradation kinetics of *Bacillus cereus* grown on phenol. J Environ Bioremediation Toxicol. 2014;2(1):1–5.